A Combined Matrix Isolation and ab Initio Study of Bromine Oxides

Oscar Gálvez,[†] Anja Zoermer,[†] Aharon Loewenschuss,[‡] and Hinrich Grothe*[,†]

Institute of Materials Chemistry, Vienna University of Technology, A-1210 Vienna, Austria, and Department of Inorganic & Analytical Chemistry, The Hebrew University of Jerusalem, Jerusalem 9190, Israel

Received: January 27, 2006; In Final Form: March 22, 2006

Bromine oxides have been generated by passing a mixture of Br_2/O_2/Ar through a microwave discharge. The products were stabilized at 6.5 K in an excess amount of argon. Infrared spectroscopy was used to analyze the species formed; experiments with enriched $^{18}O_2$ and ab initio calculations were carried out to assist in the assignment of the spectra. Besides the known species BrO, OBrO, and BrBrO, spectroscopic evidence for BrOBrO, $BrBrO_2$, and a new isomer of Br_2O_3 is reported for the first time. Extensive comparisons are drawn between the present studies and previous experimental and theoretical works. The chemistry involved in the production of the observed compounds is discussed. The assignments are corroborated by the good correlation between observed and calculated band positions and intensities.

I. Introduction

The halogen oxides, especially those containing chlorine and bromine, have received considerable attention in the last two decades, since they are involved in atmospheric processes and play a leading role in stratospheric[1,2] and tropospheric[3−5] ozone depletion reactions. Chlorine oxides have been investigated extensively for many years,[6,7] but studies on bromine oxides are much scarcer, because they are less abundant in the atmosphere and are thermodynamically less stable than the chlorine oxides. Nevertheless, during the past decade it has been shown that the bromine species have a higher ozone depletion potential than their chlorine analogues.[8,9] Enhanced concentrations of bromine species have been associated with arctic tropospheric ozone depletion episodes,[3−5] probably caused by catalytic cycles mainly involving the radicals Br and BrO, whereas the corresponding chlorine compounds were less significant in these processes.[10] Consequently, the interest in characterizing atmospheric bromine species has been stimulated in the past few years.

Most of the spectroscopic and structural information available on bromine oxides concern BrO, BrO_2 (OBrO and BrOO), and Br_2O (BrOBr and BrBrO), which are the simplest and most stable species.[11−16] The first attempts to identify these compounds date back to the 1930s, when UV−vis and IR spectroscopy helped in the identification.[17−23] For other bromine species, ab initio calculations are the major source of information.[24−30] For instance, the $(BrO)_2$ oxides, which due to kinetic data should be formed in the BrO self-reaction, are only suggested by theoretical studies which have presented respective structures and vibrational spectra;[24,25] however, they were not yet observed experimentally. Several studies, mainly on solid phases, refer to higher oxides of bromine, BrO_x ($x = 3-4$), Br_2O_y ($y = 3-7$), and Br_3O_z ($z = 6, 8$), but for some of them, their existence was not even definitely confirmed.[13,31−33]

Regarding the production of halogen oxides, different methodologies have been employed: heterogeneous reactions on HgO,[21,38] photolysis with subsequent gas-phase reaction,[34,35] and thermolysis of precursors.[42] Because of the instability of bromine oxides, the matrix isolation technique is a necessary prerequisite for stabilization of the synthesized compounds. In this context, we want to highlight the experiments of Tevault et al., in which several bromine oxygen compounds (BrO, OBrO, BrBrO, and BrOBr) were formed in an argon matrix and studied by infrared spectroscopy.[34] Subsequently, more studies have been carried out to gain insight into the nature of these oxides, mainly applying matrix isolation techniques,[35−38] but in some cases, measurements in gas phase were also successful.[39−41] However, these methods demand a certain stability of the new compound in question, and in particular, higher oxides are difficult to access. Thus, a rather harsh oxidation process and rapid stabilization at low temperatures presents itself as a viable method and results in a broad variety of products, also including hitherto unknown higher bromine oxides. Attempts to generate higher bromine oxides by passing a mixture of bromine and oxygen through a microwave or glow discharge have already been made by Pflugmacher et al. in the 1950s, resulting in different bromine species.[43] More recent experiments have produced several bromine oxides by means of the microwave discharge of Br_2/O_2 mixtures.[36,39]

In this work, we have generated bromine oxides by passing Br_2/O_2/Ar mixtures in different ratios through a microwave discharge located close to the cold surface of a cryostat kept at 6.5 K. Thus, the wide range of highly unstable bromine oxide species can, after their formation in the plasma afterglow and in the flight path to the cold surface, be stabilized in an excess amount of argon. Since the matrix layer contains a high concentration of unreacted bromine and especially oxygen atoms, further reactions of bromine species with the highly mobile oxygen is facilitated by thermal cycles, resulting in pronounced formation of higher bromine oxides. The matrix isolated species were studied by infrared spectroscopy, and the observed bands were assigned on the basis of both isotope effects due to the natural abundance of bromine isotopes and 18-oxygen enrichment as well as by comparison with results of ab initio calculations. The experimental design and the ab

* Corresponding author. E-mail: grothe@tuwien.ac.at. Tel. +43-1-25077-3809. Fax. +43-1-25077-3890.
[†] Vienna University of Technology.
[‡] The Hebrew University of Jerusalem.

10.1021/jp060586x CCC: $33.50
Published on Web 04/29/2006

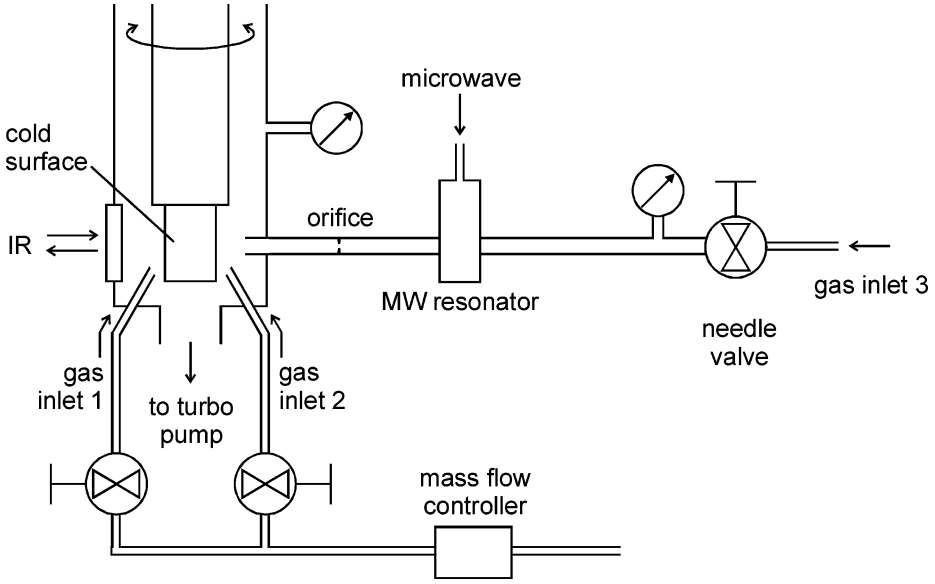

Figure 1. Matrix isolation setup for bromine oxide formation and chemistry study.

initio methods employed are addressed in the next two sections, and then, our results are reported and discussed.

II. Experimental Section

The matrix isolation setup (see Figure 1) consisted of a two-stage closed-cycle cryostat (Leybold RDK 6-320) fitted with an ultrahigh vacuum-tight shroud and rotary feedthrough for turning the sample support by 180°, i.e., from the plasma-tube side to the IR-spectrometer side and vice versa. The system allowed for extended deposition without the risk of contamination of the matrix. The base pressure of the system was below 10^{-8} mbar even during rotation. The cold surface was equipped with a silicon diode for temperature measurement and a heating unit managed by a Lakeshore 330 controller. The infrared spectrometer (Bruker 113v) was fitted with a deflection optic in one of the sample chambers to guide the beam out of the spectrometer and through a KBr window to the gold-plated sample support, thus facilitating measurement in reflection−absorption mode. The microwave discharge was effected by means of a microwave generator (EMS Microtron 200) connected to an Evenson cavity (Sairem) enclosing a quartz tube. An orifice of ca. 1.2-mm diameter downstream of the cavity ensured suitable pressures in both the plasma and the cryostat compartment. Gas samples were premixed in a separate glass vacuum line. The resulting gas consisted of 0.5% bromine (Aldrich; purified by fractioned condensation) and 0.5−1.5% oxygen ($^{16}O_2$, Linde, purity 4.5; $^{18}O_2$, Spectra Gases, 95% enriched; both gases were used without further purification) in argon (Messer, purity 6.0; used without further purification). The flow of the gas mixtures was controlled by a needle valve. Pure argon was deposited through separate inlets (gas inlets 1 and 2 in Figure 1) and controlled by a mass flow controller (MKS M330). It was found that the optical quality of the resulting matrix layers was improved when argon was co-deposited at a lower flow rate with the bromine mixtures after finishing a base layer of pure argon.

In a typical sample preparation run, a base layer of ca. 1 mmol argon was deposited at a flow rate of 1.5 mmol/h. Subsequently, the argon flow rate was turned down to 725 μmol/h, and the plasma was ignited after establishing a suitable flow of the premixed gases. The flow rate of the discharged gas was maintained at ca. 8.5 mmol/h. The quality of the resulting sample was found not to be dependent on the flow rate in the range 1−10 mmol/h. Therefore, the flow rate was kept at a value which ensured optimum working conditions for the microwave cavity. The incident microwave power was 35 W in all experiments, and the reflected power was between 4 and 9 W, depending on the gas mixture employed. The deposited amount of discharged $Br_2/O_2/Ar$ mixture was ca. 35 mmol, together with another ca. 3 mmol of pure argon. Spectra were taken at a resolution of 0.3 cm^{-1}, and 400 scans were coadded to obtain a good signal-to-noise ratio despite the low IR intensities of the bromine oxide species. All depositions were done at 6.5 K, and each matrix was subjected to a temperature cycle of 15 min at 33 K with a heating rate of 1 K/min; subsequent measurement was done at 6.5 K.

III. Calculations

Quantum calculations were performed with the hybrid DFT method B3LYP, which consists of a mixture of Hartree−Fock (HF) exchange with Becke's three parameters exchange functional plus the nonlocal correlation functional of Lee, Yang, and Parr. We chose the aug-cc-pVTZ basis set as a fair compromise between size and reliability. DFT calculations with a sufficiently flexible basis have been found well-suited to obtain geometries,[25] spectra,[27] and heats of formation[26] of bromine oxides. Equilibrium geometries were fully optimized using analytic gradients without symmetry constraints. The energies for every structure used in the calculations of reaction energies include the zero-point energy correction (ZPEC). Geometries, frequencies, and energies were determined with the *Gaussian 03* package.[44]

IV. Results

Matrix Isolation Experiments. Different ratios of Br_2/O_2 (1:1, 1:2, and 1:3) were discharged and co-deposited in an argon matrix. After deposition, infrared absorptions were measured in the spectral range 500−4000 cm^{-1}. However, most bromine oxides can be observed in the region 650−950 cm^{-1} as shown in Figure 2. When the matrix is subjected to an annealing process, concentrations of the species previously observed undergo strong changes, and new absorption bands are also recorded. The amount of ozone (band labeled O in the spectra)

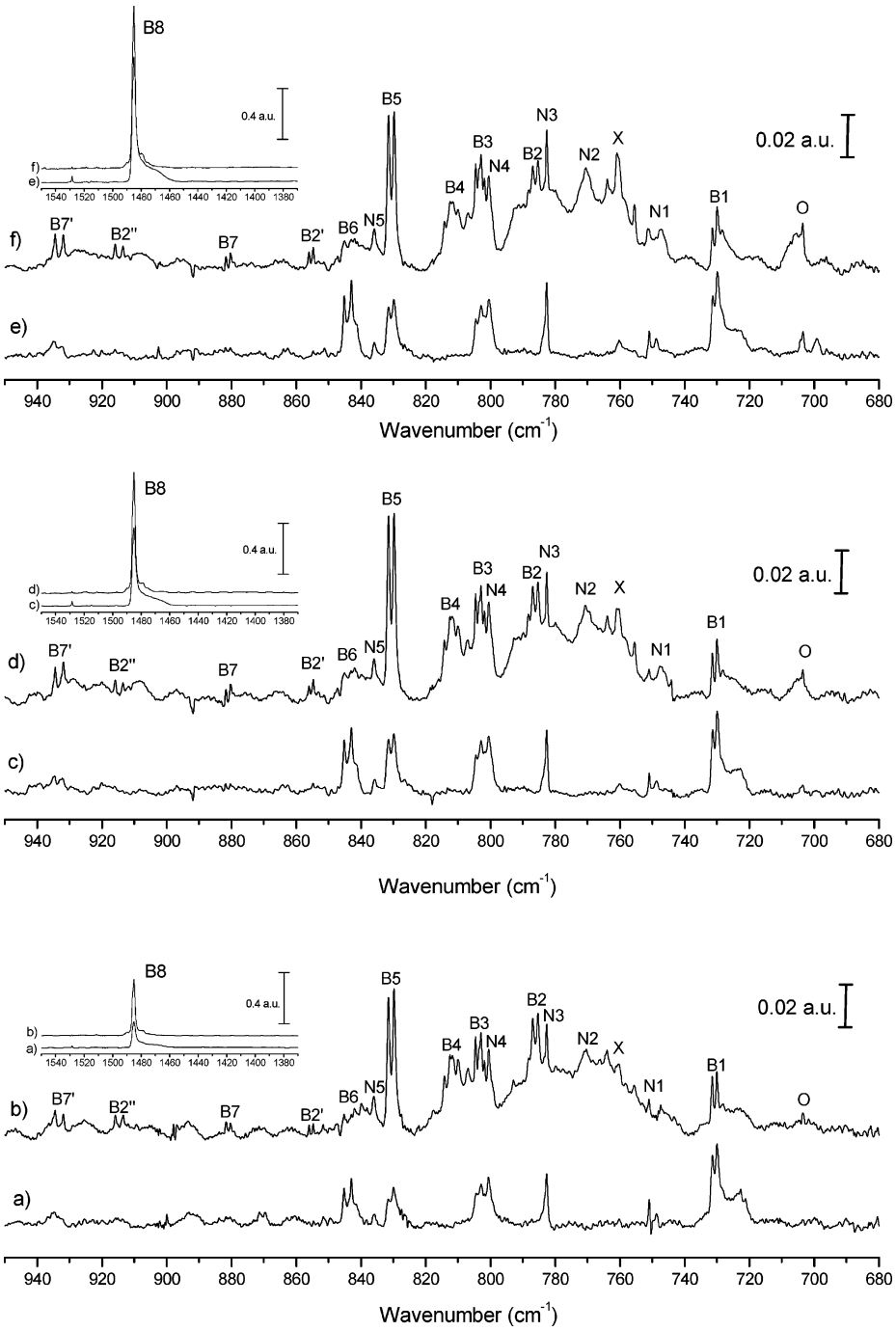

Figure 2. Infrared spectra observed following the deposition of microwave-discharged bromine and 16-oxygen mixture in argon matrixes. (a, c, e) $Br_2/^{16}O_2$ ratio of 1:1, 1:2, and 1:3, respectively. (b, d, f) Previous matrixes after annealing for 15 min at 33 K.

and the bands N2 and N5 increase. We use the label "N" for addressing species containing nitrogen atoms (its origin is explained in the discussion section) and "B" to refer to bromine oxides. Concerning the bromine species, B1 decreases and B6 vanishes after annealing. The bands B3, B5, and B8 increase, and six new bands appear: B2, B2′, B2″, B4, B7, and B7′ (labels with the same number refer to different vibrational modes of the same molecule). When the ratio of bromine/oxygen is changed, different abundances of the species can be observed. Consequently, the concentration of ozone formed during annealing increases with the amount of oxygen in the sample. Species which contain nitrogen atoms also show larger concentration when the amount of oxygen in the mixture is higher. The bromine species (B1 to B8 in the spectra) show different behaviors when the ratio Br_2/O_2 is altered. The group of bands B1, B3, B5, B6, B7, B7′, and B8 increase in intensity when the ratio changes from 1:1 to 1:2, but stay nearly constant from 1:2 to 1:3. B2 remains almost invariable despite the different amounts of oxygen in the mixture, and the band B4 increases from 1:1 to 1:2 and decreases when the ratio of bromine/oxygen is 1:3. The low intensity of the bands B2′ and B2″ makes it rather difficult to properly analyze their variations.

To help in the assignment of the bands, similar experiments with 18-oxygen were carried out, and the spectra are shown in Figure 3. All the positions of bands shown in Figure 2 are red-shifted in different proportions, verifying the absence of species not containing oxygen. Because of the different red-shifts, the pattern of the infrared bands shows some differences with respect to those with 16-oxygen. Band N4 is shifted to the higher-wavenumber side of B3, at 773.0 cm^{-1}, overlapping with

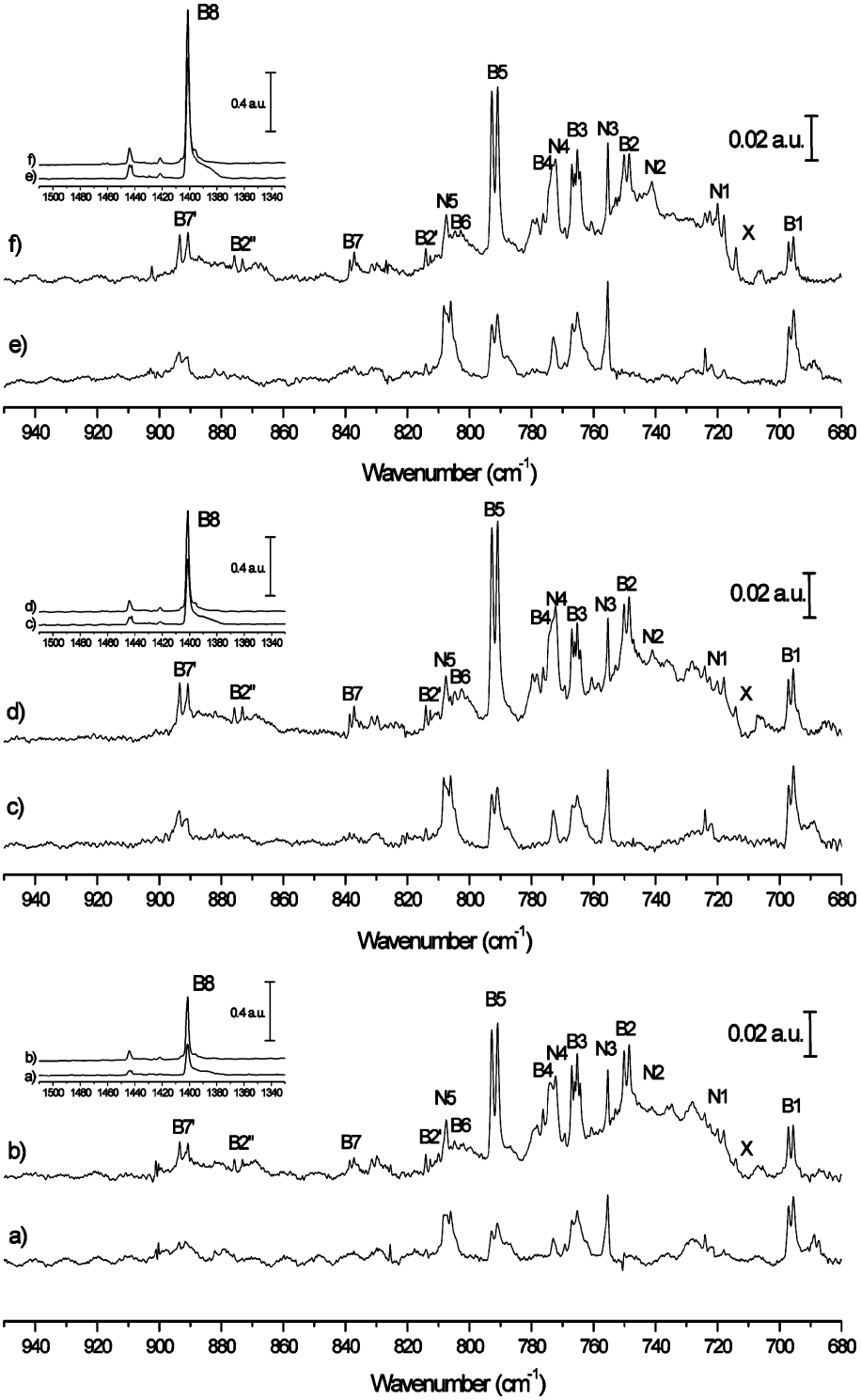

Figure 3. Infrared spectra observed following the deposition of microwave-discharged bromine and 18-oxygen mixture in argon matrixes. (a, c, e) $Br_2/^{18}O_2$ ratio of 1:1, 1:2, and 1:3, respectively. (b, d, f) Previous matrixes after annealing for 15 min at 33 K.

B4, while N5 and B6 are also in the same frequency range in the spectra. Regardless of these differences, the 18-oxygen bands show variations similar to those of the 16-oxygen bands described before when the matrix is annealed or the ratio $Br_2/^{18}O_2$ is changed. All band positions shown in Figures 2 and 3 are listed in Table 1.

Ab initio Calculations. The infrared spectra recorded are very congested in the region of interest for the identification of bromine oxide species. For several of these species, no previous infrared spectroscopic information is available, so quantum chemical methods can be of appreciable help in understanding the observed spectra. We provide in Table 2 B3LYP calculations of the geometrical parameters and harmonic frequencies for bromine species supposed to be formed in our experiments along with the available theoretical and experimental data found in the literature. High-level ab initio results from other authors, mostly obtained with MP2 and CCSD(T) methods, have been included in Table 2 for the purpose of comparison. In some instances, DFT data similar to ours were selected when other methods were not available. The experimental data included for comparison are primarily from measurements in the gas phase, although frequency values observed in argon matrix were

TABLE 1: Wavenumbers (cm^{-1}) of the Products of a Microwave-Discharged Mixture of Molecular Bromine and Molecular 16- or 18-Oxygen, Respectively, in an Excess of Argon[a]

	IR (Ar matrix)		
band	$^{16}O_2$	$^{18}O_2$	species
C	663.5	653.6	CO_2
	661.9	651.9	
O	703.6	664.0	O_3
B1	730.1 (731.6)	695.5 (697.1)	BrO
N1	751.0	724.0	NO_2
	748.7	722.5	N_2O_4
	747.4	721.8	N_2O_4
X	763.9	718.0	X−O−O−Y
	760.3	714.0	
	755.5	706.6	
N2	769.5 (770.5)	741.2 (742.7)	$Br(ONO)_x$
N3	782.7	755.3	$BrNO_2$
B2	785.3 (787.0)	748.5 (750.2)	$OBrBrO_2$
B2′	854.7 (856.0)	812.7 (814.2)	
B2″	913.5 (915.9)	873.2 (875.8)	
B3	802.9 (804.6)	765.2 (766.9)	BrBrO
	801.9 (803.6)	764.4 (766.0)	
N4	800.5	772.9	$BrONO_2$
B4	810.0, 811.6, 812.5, 814.2	774.6, 776.3, 778.3, 779.6	BrBrO···X
B5	829.7 (831.5)	791.0 (792.8)	BrOBrO
N5	835.9	807.6	BrONO
B6	843.0 (845.3)	806.0 (808.3)	OBrO
B7	880.3 (881.7)	837.1 (838.6)	$BrBrO_2$
B7′	931.9 (934.4)	890.8 (893.4)	
B8	1485.1	1401.3	BrOO

[a] When pairs of bands are recorded, the absorption caused by the 79-bromine isotope is given in parentheses.

selected when gas-phase data do not exist. Our calculated geometrical parameters yield results similar to those of ab initio calculations from other authors, showing deviations less than 0.05 Å and 8° (3° in most cases) for bond lengths and angles, respectively. The only exception is our calculated Br−O bond length for the BrOO molecule, which shows large differences from the calculations of other authors.[29] In this case, the bromine−oxygen interaction is weak, and consequently, the bond length is large, making proper calculations difficult and resulting in discrepancies among different ab initio methods. The B3LYP results are in good agreement with the experimental data available, with differences less than 0.05 Å and 3° in bond lengths and angles, respectively. Ab initio results generally overestimate the vibrational frequency values due to the neglect of anharmonic corrections. Nevertheless, in the majority of cases, our B3LYP calculations yield smaller values than MP2, showing better agreement with the experimental values obtained by others groups, with deviations typically less than 3%.

V. Discussion

Contrary to other experiments described in the literature, which were designed to yield some specific bromine oxide,[37,38] our method of production generates a high number of different species. As mentioned before, this fact could complicate the assignment of the IR spectra; nevertheless, our method provides the opportunity to form species not previously studied, for instance, the BrO dimers. Bromine oxides usually show less infrared activity than the analogous chlorine compounds; e.g., BrO has an absorption coefficient two times lower than that of ClO.[57,58] Although this fact introduces yet another complication to getting high-quality spectra, infrared spectroscopy remains the method of choice, because it provides information about the geometry of the compounds and thus assists the proper assignment of the bands. The observation of reactions inside the matrix during thermal cycles, confirmed by the respective changes in band intensities and the appearance of new bands, supports our assignments, as will be discussed in the following sections.

Spectra after Deposition of the Discharged Mixture. The spectra recorded immediately after deposition of the discharged mixture (Figures 2 and 3) show characteristic bands, which can be classified into pairs of bands and single bands. Bromine has two natural isotopes in almost equal amounts (50.54% for ^{79}Br and 49.46% for ^{81}Br), and consequently, with sufficient resolution, band pairs are expected for modes which involve movements of one bromine atom. The origin of the single bands recorded will be discussed in detail later. Bromine and oxygen atoms are formed in the plasma tube after the microwave discharge and react to generate the different compounds observed in the spectra. Besides IR-inactive species such as Br_2 and O_2, bromine monoxide could be expected as the major product in this reaction, although Br_2O, BrO_2, and different dimers of BrO are other probable species.

Four pairs of bands related to bromine oxides are observed before annealing: B1, B3, B5, and B6. In former experiments by Tevault et al.,[34] bands similar to B1, B3, and B6 were observed and assigned to BrO, BrBrO, and OBrO molecules, respectively. The frequency values recorded by Tevault for these bands deviate from our values at less than 1 cm^{-1} for BrO and BrBrO, but 7 cm^{-1} for OBrO. Kölm et al.[37] and Maier and Bothur[59] observed the asymmetric stretching mode of OBrO at 845.2 and 846.6 cm^{-1}, respectively, differing from our observation by less than 1 cm^{-1}, so the value of Tevault for OBrO should presumably be considered with some caution. The measured and calculated frequency values and intensities for these compounds are summarized in Table 3. Although anharmonic corrections are not included in the calculations, frequencies deviate less than 3% from the measurements. The symmetric stretching mode of OBrO was observed at 795.7 cm^{-1} by Kölm[37] and at 794.1 cm^{-1} by Maier and Bothur.[59] According to our B3LYP calculation (results not shown), this normal mode is 10 times less intense than the asymmetric stretching, so this band may be too weak to be observed in our spectra. The calculated and observed shifts due to the natural bromine isotopes show exactly the same values: 1.5, 1.7, and 2.3 cm^{-1} for the B1, B3, and B6 species, respectively. The analogous shifts caused by 16- and 18-oxygen isotopes for these species are 34.5, 37.5, and 37.0 cm^{-1}, which is also in good concordance with our calculated values of 35.2, 39.2, and 38.5 cm^{-1}. B1 shows a shoulder at ca. 723 cm^{-1} (689 cm^{-1} with 18-oxygen) which might be caused by a complex X···BrO. This band decreases when the matrix is annealed, so a small molecule, which can move inside the matrix, could be involved in this complex. Our ab initio calculations for hydrates of BrO show a red-shift of 10 cm^{-1} for a complex H_2O···BrO (publication in process). Typical absorptions due to the O−H stretch in water molecules are also recorded in the region between 3700 and 3800 cm^{-1}, so we tentatively assign the shoulder to this complex. In the region of the stretching −Br−O mode of BrBrO, four bands (labeled B3) with different intensities can be observed in the experiments with 18-oxygen, along with a group of five bands in the 16-oxygen spectra due to the absorption of species N4, which will be discussed toward the end of this section. There are four different possibilities of combining the two natural bromine isotopes to yield BrBrO, which all have almost the same probability. Nevertheless, the Br isotope splitting is not expected for ν(Br−O), since the BrO

TABLE 2: Ab Initio Geometric Parameters and Vibrational Frequencies in Comparison with Calculated and Experimental Literature Values[aa]

species	parameter	B3LYP this work	ab initio other authors	exptl	species	parameter	B3LYP this work	ab initio other authors	exptl
BrO	r(Br−O)	1.729	1.743[a]	1.717[c]	$OBrBrO_2$	r(O−Br-)	1.695		
	stretch BrO	742.0	784[b]	723.4[d]		r(−Br−Br-)	2.763		
BrO_3	r(Br−O)	1.634	1.604[e]			r(−Br−O_{cis})	1.631		
	θ(O−Br−O)	112.4	114.0[e]			r(−Br−O_{trans})	1.635		
	stretch sy Br−O_3 (A)	801.8	815[f]	800[g]		θ(O−Br−Br-)	108.5		
	stretch asy Br−O_3 (E)	788.0	810[f]	828[g]		θ(−Br−Br−O_{cis})	101.9		
BrBrO	r(Br−Br)	2.427	2.45			θ(−Br−Br−O_{cis})	99.1		
	r(Br−O)	1.674	1.64[h]			τ(O−Br−Br−O_{cis})	−46.3		
	θ(Br−Br−O)	111.3	112.8[h]			stretch O−Br-	797.9		
	stretch −Br−O	827.3	1056[h]	804.6[i]		stretch sy −Br−O_2	860.5		
BrOBrO	r(Br−O-)	1.858	1.846[j]			stretch asy −Br−O_2	922.9		
	r(−O−Br-)	1.868	1.904[j]		$Br-NO_2$	r(Br−N)	2.057	2.040[q]	2.012[r]
	r(−Br−O)	1.663	1.630[j]			r(−N−O)	1.188	1.201[q]	1.196[r]
	θ(Br−O−Br-)	116.8	111.6[j]			θ(Br−N−O)	114.0	114.3[q]	114.5[r]
	θ(−O−Br−O)	110.3	112.0[j]			θ(O−N−O)	131.9	131.4[q]	131.0[r]
	τ(Br−O−Br−O)	78.4	70.3[j]			τ(Br−N−O−O)	180.0	180.0[q]	180.0[r]
	stretch −Br−O	850.8	1082[b]			scissors −NO_2 (A1)	804.7	799[q]	782.9[s]
OBrO	r(O−Br)	1.652	1.656[a]	1.649[k]	*trans*-BrONO	r(Br−O-)	1.836	1.849[q]	
	θ(O−Br−O)	113.9	117.5[a]	114.4[k]		r(−O−N-)	1.503	1.529[q]	
	stretch sy BrO_2 (A_1)	828.5	877[b]	799.4[l]		r(−N−O)	1.150	1.158[q]	
	stretch asy BrO_2 (B_2)	869.1	898[b]	848.6[l]		θ(Br−O−N-)	111.1	108.4[q]	
BrOO	r(Br−O-)	2.512	2.258[m]			θ(−O−N−O)	108.5	108.1[q]	
	r(−O−O)	1.199	1.168[m]			τ(Br−O−N−O)	180.0	180.0[q]	
	θ(Br−O−O)	118.4	118.3[m]			bend −O−N−O (A′)	865.1	835[q]	835.9[t]
	stretch −O−O	1585.6	1581[m]	1485.1[i]	$BrONO_2$	r(Br−O-)	1.837	1.821[u]	1.829[v]
$BrOBrO_2$	r(Br−O-)	1.829	1.840[n]			r(−O−N-)	1.485	1.502[u]	1.456[v]
	r(−O−Br-)	1.916	1.971[n]			r(−N−O_{cis})	1.189	1.190[u]	1.205[v]
	r(−Br−O)	1.615	1.623[n]			r(−N−O_{trans})	1.191	1.193[u]	1.205[v]
	θ(Br−O−Br-)	114.8	113.6[n]			θ(Br−O−N-)	115.1	113.0[u]	113.9[v]
	θ(−O−Br−O)	104.1	101.2[n]			θ(−O−N−O_{cis})	118.0	117.4[u]	119.5[v]
	τ(Br−O−Br−O)	55.9				θ(−O−N−O_{trans})	109.2	108.6[u]	106.6[v]
	stretch sy −Br−O_2 (A′)	905.3	911°			τ(Br−O−N−O_{cis})	0.0	0.0[u]	0.0[v]
	stretch asy −Br−O_2 (A″)	953.8	966°			stretch Br−O− (A′)	751.5	753[u]	750[w]
$BrBrO_2$	r(Br−Br-)	2.495	2.488[j]			scissors −NO_2 (A′)	815.1	780[u]	803.3[u]
	r(−Br−O)	1.620	1.595[j]						
	θ(Br−Br−O)	104.4	104.1[j]						
	θ(O−Br−O)	111.3	112.1[j]						
	τ(Br−Br−O−O)	112.0							
	stretch sy −Br−O_2 (A′)	887.2	893[p]						
	stretch as −Br−O_2 (A″)	942.8	950[p]						

[aa] Bond distances, r, in Å; angles, θ and τ, in deg; and frequencies in cm^{-1}. For the harmonic frequencies calculation, ^{79}Br, ^{16}O, and ^{14}N isotopes were used. [a] MP2/6-311G* in ref 30. [b] MP2/6-31G* in ref 30. [c] Ref 11. [d] Gas phase in ref 45. [e] MP2/6-311G(2df) in ref 46. [f] B3LYP/6-311G(2df) in ref 46. [g] Deduced from an assumed geometry for BrO_3 in ref 47. [h] MP2/6-31G(3d1f) for O and (9s,6p,2d) contraction of a (14s,11p,5d) primitive set with additional set of d and f polarization functions for Br, in ref 38. [i] Ar matrix in ref 38. [j] MP2/AREP/TZ(2df) in ref 24. [k] Ref 48. [l] Ref 49. [m] MP2/AREP/TZ(2df) in ref 29. [n] B3LYP/DZP++ in ref 28. [o] B3LYP/6-311+G(3df) in ref 27. [p] B3LYP/6-311++G(3df,3dp) in ref 25. [q] CCSD(T)/TZ2P in ref 50. [r] Ref 51. [s] Ar matrix in ref 52. [t] Ar matrix in ref 53. [u] MP2/6-311++G(3df) in ref 54. [v] Ref 55. [w] Ne matrix in ref 56.

TABLE 3: Observed and Calculated IR Frequencies of the Br−O Stretching Modes of the Bromine Oxides Studied in This Work[a]

	calculation (B3LYP this work)					IR Ar matrix				
species	^{79}Br, ^{16}O	^{81}Br, ^{16}O	^{79}Br, ^{18}O	^{81}Br, ^{18}O	intensity[b]	^{79}Br, ^{16}O	^{81}Br, ^{16}O	^{79}Br, ^{18}O	^{81}Br, ^{18}O	assignment
BrO	742.0	740.5	706.8	705.3	1	731.6	730.1	697.1	695.5	stretch Br−O
BrBrO	827.3	825.6	788.1	786.4	61	804.6	802.9	766.9	765.2	stretch Br−O
BrOBrO	850.8	849.0	810.7	808.9	65	831.5	829.7	792.8	791.0	stretch −Br−O
OBrO	869.1	866.8	830.6	828.2	49	845.3	843.0	808.3	806.0	asym stretch BrO_2
$OBrBrO_2$	797.9	796.3	760.0	758.3	131	787.0	785.3	750.2	748.5	stretch O−Br-
	860.5	859.2	817.6	816.2	78	856.0	854.7	814.2	812.7	sym stretch −BrO_2
	922.9	920.4	882.0	879.3	86	915.9	913.5	875.8	873.2	asym stretch −BrO_2
BrBrOO	887.2	885.8	842.8	841.4	76	881.7	880.3	838.6	837.1	sym stretch −BrO_2
	942.8	940.2	900.8	898.2	97	934.4	931.9	893.4	890.8	asym stretch −BrO_2

[a] Frequencies in cm^{-1} and intensities in km/mol. [b] Calculated at B3LYP/aug-cc-pVTZ.

vibration is weakly coupled with the low-lying Br−BrO mode. Accordingly, the four maxima shown in the absorption of B3 are presumably caused by matrix splitting due to different environments. From our calculated intensity values (see Table 3), BrBrO and OBrO are about 50 times stronger IR absorbers than BrO. Despite this, the band B1 shows higher intensity in the spectra than B3 and B6, so the concentration of BrO in the matrix must be much higher, in accord with our assumption of BrO being the dominant species. In the region of the O−O stretching vibrations, a band (B8) at 1485.1 cm^{-1} was recorded. This band was previously observed by different groups and assigned to the O−O stretching mode of the BrOO molecule.[34,37]

Another pair of bands is observed around 830 cm^{-1} (792 cm^{-1} for the experiments with $^{18}O_2$) before the annealing process, and was formerly tentatively assigned by Tevault et al.[34] to $(BrO)_2$. This compound has been proposed to exist as an important intermediate in the BrO self-reaction

$$BrO + BrO \rightarrow [(BrO)_2^*] \rightarrow Br_2 + O_2 \qquad (1)$$

which is the key step in the catalytic destruction of tropospheric ozone occurring in the arctic vortex during springtime (see ref 10 and references therein). Despite the importance of $(BrO)_2$, no conclusive spectroscopic information is available so far to confirm its existence. Since BrO is the major bromine oxide species formed after reaction of bromine and oxygen atoms, reaction 1 could probably take place, and the dimer could be stabilized in the argon matrix. Three different dimers can be proposed as the product of this reaction

$$BrO + BrO \rightarrow BrOOBr \quad \Delta E = -16.93 \text{ kcal/mol} \quad (2)$$

$$\rightarrow BrOBrO \quad \Delta E = -6.08 \text{ kcal/mol} \quad (3)$$

$$\rightarrow OBrBrO \quad \Delta E = +13.44 \text{ kcal/mol} \quad (4)$$

The values for ΔE are calculated including the ZPEC as outlined in section III. While the formation of BrOOBr (reaction 2) and BrOBrO (reaction 3) are thermodynamically favored, the production of OBrBrO (reaction 4) is an endothermic process. The calculated vibrational frequencies, with a correction factor of 0.986 for taking anharmonic effects into account, show an infrared absorption around 830 cm^{-1} for BrOOBr and BrOBrO. In the case of BrOOBr, this IR absorption is caused by the O−O stretching mode, so bromine isotopic splitting is not expected. Our calculations also predict another intense IR absorption at 586 cm^{-1} for this species, which is not observed in our spectra. As a consequence of these facts, we tentatively assign the band B5 to the stretching −Br−O normal mode of BrOBrO, in good accordance with our predicted value (see Table 3). The calculated bromine and oxygen isotopic splittings for this normal mode are 1.8 and 40.1 cm^{-1}, which is in very good agreement with the measured values of 1.8 and 38.7 cm^{-1}. The other stretching and bending modes of this compound are below the low-frequency limit of our setup. The presence of $(BrO)_2$ with the structure BrOBrO agrees with recent experiments of Odeh et al. studying the reaction $BrCl + ClO_2^-$.[60] The authors propose that the reaction proceeds through BrOXO intermediates with a chainlike structure rather than a Y-shaped form. In high theoretical level calculations, the nonplanar linear conformation of BrOBrO yields the highest interaction energy, with differences larger than 3 kcal/mol with respect to the other conformations.[30] These findings support our structural assignments. The compound $BrBrO_2$, which presents a Y-shaped structure, is also found in our experiments (see bands B7 and B7′ in the spectra), but it is probably not formed in the course of the BrO self-reaction, as will be discussed in more detail later.

To elucidate the origin of the single bands, experiments with mixtures enriched in possible contaminants (nitrogen, carbon, and hydrogen) were carried out. When ca. 10% of N_2 is added to the mixture (results not shown), bands labeled "N" in our spectra are dramatically increased in intensity. This fact reveals that these absorptions belong to species containing nitrogen. These contaminations most probably arise from impurities of the gases used for the mixtures. The most likely source is O_2, because the amount of nitrogen species increases with the amount of oxygen in the mixture. By comparison with IR spectra recorded in argon matrix and reported in the literature, the bands N1, N3, N4, and N5 could be assigned to bending modes of $-NO_2$ groups in the species NO_2,[61] $BrNO_2$,[52] $BrONO_2$,[56] and *trans*-BrONO,[53] respectively. These assignments agree with our calculated frequencies for these molecules, displaying deviations less than 4% (see Table 2). In the case of the NO_2 band, several maxima are observed. We assign the maximum at 751.0 cm^{-1} to pure NO_2 and the maxima at 748.7 and 747.4 cm^{-1} to N_2O_4 species, according to the experiments of Louis and Crawford.[62] Our predicted intensity values for the nitrogen-containing species (with the exception of NO_2) are 2 orders of magnitude higher than bromine monoxide. Although the intensities of these bands, especially N3 and N4, appear comparable with those of the bromine oxides, the concentrations of these species in our matrix are rather low. Experiments with mixtures enriched in CO and water were also done, but no relevant features were found in the spectral region under study, revealing that impurities of carbon and hydrogen are not responsible for the formation of the bands shown in the figures. When the amount of oxygen in the mixture is increased, a low-intensity group of bands grows (bands labeled "X" in the spectra), with the strongest absorption at 760.3 cm^{-1}, which is red-shifted to 718.0 cm^{-1} in the experiments with 18-oxygen. These bands neither show the natural bromine isotopic splitting nor increase when contaminants are deliberately added to the mixture, so we tentatively suggest that O−O stretching vibrations in higher bromine peroxides could be the modes responsible for these absorptions.

Spectra after Annealing Process. When an ideal and extremely dilute matrix is subjected to an annealing process, the structure relaxes and the argon atoms are reordered to yield the face-centered cubic structure of the equilibrium rare-gas solids.[63] This fcc structure is usually not completely achieved in a real matrix due to the disorder generated by the guest molecules. During the process of annealing, small species can move inside the matrix and react with larger molecules embedded in it. In this process, an excess of oxygen atoms produced in the microwave discharge and deposited in the argon matrix could react with bromine species, yielding higher bromine oxides. This idea is supported by the increase of ozone formed by the reaction of O_2 and oxygen atoms during annealing (see Figure 2), revealing the presence of unreacted oxygen atoms in the matrix environment. The voluminous bromine compounds are not expected to become mobile, so reactions are facilitated by small mobile species, in particular, oxygen atoms.

The concentration of BrO (band B1) decreases during annealing, most probably due to reactions inside the matrix leading to other compounds. Assuming that BrO is reacting with oxygen atoms, two possible products could be generated

$$OBr + O \rightarrow OBrO \quad (5)$$

$$BrO + O \rightarrow BrOO \quad (6)$$

Reaction 5 does not seem to occur to a large extent, because the OBrO band (B6) nearly disappears during annealing. Nevertheless, a strong increase in the intensity of the O−O stretching vibration of BrOO (band B8) is observed, supporting the second reaction channel. A higher excess of oxygen atoms is expected when the amount of oxygen in the mixture is elevated, and consequently, a larger decrease of BrO should be observable in mixtures rich in oxygen. This assumption agrees with the results obtained by the evaluation of the BrO band areas in Figures 2 and 3, which show a 30% larger decrease of this band for a ratio of Br_2 to O_2 of 1:3 in comparison to 1:1.

The concentration of BrBrO (B3) increases during the thermal cycle. This fact could be caused by the reaction of IR-inactive molecular bromine with oxygen atoms. When a large excess of oxygen is available (i.e., in mixture 1:3), more bromine is expected to be consumed already in the microwave discharge, depleting the final concentration inside the matrix. Consequently, a minor increase of the BrBrO concentration is expected for oxygen-rich mixtures. This correlation is found in our experiments, offering support to our assumptions.

The band belonging to BrOBrO (B5) dramatically increases in intensity during annealing. Since BrO is immobilized after

it is embedded in the matrix, the BrO self-reaction is no viable path for the formation of BrOBrO during the thermal cycle. A possible reaction to form BrOBrO inside the matrix would be

$$\mathrm{BrOBr} + \mathrm{O} \rightarrow \mathrm{BrOBrO} \quad (7)$$

The symmetric and asymmetric stretching modes of BrOBr have been observed by Kölm et al.[37] in argon matrix at 622.2 and 525.3 cm^{-1}, respectively. Because both the experimental intensities for these modes are much lower than those of the compounds described before and our setup shows very low signal intensity below 650 cm^{-1}, we do not observe this oxide in our spectra. Our calculated intensities confirm the low values for these two normal modes of BrOBr, being around 40 and 15 times lower than the −Br−O stretching mode of BrBrO and BrOBrO, respectively. Thus, we can only assume reaction 7 as the most probable path for the formation of BrOBrO.

The concentration of OBrO drastically decreases in the annealing process, although reaction 5 would be a possible path to form OBrO molecules. Following the chemistry described for the other species, oxygen atoms could react with OBrO to produce BrO_3. While many authors have claimed to find BrO_3,[43,47] no definite experimental evidence of this radical has been reported so far. Several theoretical studies have been performed to elucidate the structure and IR frequencies.[24,46] Although this compound is expected to have two IR absorptions in the region under study (see Table 2), we have not observed any band which could confidently been ascribed to BrO_3 with the predicted C_{3v} structure. Nevertheless, further experiments have to be performed to consider other possible structures of BrO_3.

Six new pairs of bands ($^{79/81}$Br) become visible after the annealing process: B2, B4, B2′, B2″, B7, and B7′. To elucidate the origin of these bands, we have calculated the structures and harmonic frequencies of different compounds which might be formed in the reaction between the species previously identified in the matrix and oxygen atoms, namely, BrO_3, OBrBrO, OBrOBrO, $BrOBrO_2$, $BrBrO_2$, $BrBrO_3$, $OBrBrO_2$, $OBrOBrO_2$, and $BrOBrO_3$. We tentatively assign the set of bands B7 and B7′ to the symmetric and asymmetric stretching $-BrO_2$ modes of $BrBrO_2$. There are no previous experimental data for this species, although several theoretical works have been done to elucidate its structure and vibrational frequencies.[24,25] In addition to the small amount of $BrBrO_2$ formed immediately after the microwave discharge, probably produced by the reaction of Br_2 and O_2, a possible way to generate it during the annealing is described by the following reaction:

$$\mathrm{BrBrO} + \mathrm{O} \rightarrow \mathrm{BrBrO_2} \quad (8)$$

Thus, BrBrO is generated as well as consumed during the thermal cycle. Our calculated frequencies for $BrBrO_2$ deviate less than 1% from the recorded values. The bromine isotopic splittings observed are 1.4 and 2.5 cm^{-1} for B7 and B7′, which is in very good concordance with our calculated values of 1.4 and 2.6 cm^{-1}. The observed red-shifts introduced by 18-oxygen are 43.1 and 41.0 cm^{-1} for B7 and B7′, in good agreement with our calculated values of 44.4 and 42.0 cm^{-1}, respectively. Our predicted intensities (see Table 3) show a stronger absorption for the asymmetric mode, as is observed in our spectra. To evaluate the splitting caused by the break of the symmetry in the stretching modes of $-BrO_2$, an experiment with a mixture of 16- and 18-oxygen was carried out. The spectrum recorded presents a "forest of bands" in the region under study. Since most of these bands do not add new information to our discussion, the spectra are not shown, and we will only mention features relevant for our assignments. The spectrum recorded in the experiment with a mixture of $^{16}O_2$ and $^{18}O_2$ reveals a new band which shows a red-shift of 13.4 cm^{-1} with respect to B7′, in very good agreement with our simulated spectrum of $BrBr^{16}O^{18}O$, which yields a red-shift of 13.8 cm^{-1} for this absorption.

The bands around 786 cm^{-1} (B2) were already observed by Tevault et al. and assigned to a complex BrBrO···X. According to our calculated spectra for $OBrBrO_2$, the stretching O−Br− mode of this molecule shows a predicted harmonic value of 797.9 cm^{-1}, which compares well with the recorded value for B2. A possible way for the formation of this compound in the matrix involves the following sequence:

$$\mathrm{Br_2} + \mathrm{O} \rightarrow \mathrm{BrBrO} \quad (9)$$

$$\mathrm{BrBrO} + \mathrm{O} \rightarrow \mathrm{BrBrO_2} \quad (8)$$

$$\mathrm{BrBrO_2} + \mathrm{O} \rightarrow \mathrm{OBrBrO_2} \quad (10)$$

Unreacted molecular bromine as well as BrBrO are present in the matrix in appreciable amounts before annealing and thus provide the educts for the formation of $OBrBrO_2$. The small amount of $BrBrO_2$ observed immediately after the microwave discharge could also facilitate the formation of this compound. Previous theoretical and experimental information has not been found for $OBrBrO_2$, but different studies proved the existence of $BrOBrO_2$.[31,64] The latter, the mixed anhydride, can be synthesized in solution and is stable in the solid phase and might be present in minor amounts also in our experiments. However, processes in matrix are dominated by kinetic and steric effects rather than thermodynamics. Thus, unusual species are often observed in matrix isolation spectroscopy. The band pair B2 shows a bromine isotopic splitting of 1.7 cm^{-1}, which agrees well with the calculated value for the stretching O−Br− mode of $OBrBrO_2$ of 1.6 cm^{-1}. The oxygen isotopic splitting observed for this band is 36.8 cm^{-1}, which is also in good concordance with the predicted value of 37.9 cm^{-1}. $OBrBrO_2$ further has two intense normal modes in the region of the spectra shown in the figures. The calculated frequency values for the symmetric and asymmetric stretching $-BrO_2$ modes are around 860 and 923 cm^{-1}, which fit well with the recorded values for B2′ and B2″ (see Table 3). The predicted intensities for these modes are noticeably lower than for the O−Br− stretching vibration, a feature which is also observed in the recorded spectra. In addition to these facts, the calculated bromine isotope splittings for these modes are 1.3 and 2.5 cm^{-1}, which is in good agreement with the recorded values of 1.3 and 2.4 cm^{-1}. The calculated oxygen isotopic shifts of 42.9 and 40.9 cm^{-1} also agree with the measured values of 41.8 and 40.1 cm^{-1}. The predicted pattern for the stretching O−Br− and $-BrO_2$ modes of $OBrBrO_2$ in a mixture of $^{16}O_2/^{18}O_2$ could not properly be observed in our spectrum, since the low intensity of the bands and the overlapping with other absorptions complicate the analysis. We also like to mention that our calculated frequencies for the symmetric and asymmetric stretching $-BrO_2$ modes of $BrOBrO_2$, which was claimed to be a product of the reaction of bromine with ozone at −50 to −60 °C,[31] have similar values to those from $OBrBrO_2$ (see Table 2). Nevertheless, the agreement of the calculations with the measured bands B2′ and B2″ is worse for $BrOBrO_2$ than for $OBrBrO_2$. Additionally, the difference between the experimental and calculated values of the symmetric and asymmetric stretching mode of $-BrO_2$ would point to different anharmonicities in the case of $BrOBrO_2$, which

renders this compound even less likely. Taking all these findings into account, we assign the bands B2, B2′, and B2″ to the molecule $OBrBrO_2$; nevertheless, some uncertainty remains. Finally, the band group B4, for which additional information has not been found in the literature, was tentatively assigned to a BrBrO complex. The four bands belonging to B4 suggest a matrix splitting as for BrBrO (B3); in the 18-oxygen spectra, the bands are overlapping with the absorption of $BrONO_2$, changing the original shape of this band group. Nevertheless, we do not have enough information to complete a conclusive assignment for these bands, and further investigations are needed.

VI. Conclusion

We have studied the bromine oxides formed after microwave discharge of a mixture of bromine and oxygen in different ratios. Bromine oxides are relevant compounds which are involved in the process of stratospheric and tropospheric ozone depletion and are less stable than the analogous chlorine oxides. The species formed in the reaction were stabilized in an excess of argon and deposited on a cold surface kept at 6.5 K by a cryostat. When the matrix is subjected to a thermal cycle, unreacted oxygen atoms embedded in the matrix become mobile and react with trapped bromine species, thus facilitating further reactions inside the matrix. The products embedded in the argon matrix were studied by infrared spectroscopy. Our method of production yields a large variety of bromine oxides. Despite the complications of dealing with spectra with a high number of absorptions, this method generates species not previously reported. Mixtures deliberately enriched in contaminant species, isotopic exchange experiments, and ab initio calculations were employed to assist in the assignment of the spectra. Our calculated frequencies for the compounds proposed are in good agreement with the observed bands. The calculated shifts for the two natural bromine isotopes and the 18-oxygen experiments also are in very good concordance with our recorded values. These results support our assignments and conclusions.

The major infrared-active compound formed in the reaction is BrO, which might be overlooked due to its very low absorption intensity. In addition, OBrO, BrOO, BrBrO, and BrOBr are generated after the microwave discharge. Because of the high concentration of BrO, the self-reaction of this compound takes place before it is immobilized in the matrix, generating BrOBrO as the dominant product. BrOBr is not observed in our spectra because of its low infrared activity, but is most probably present since BrOBrO is also formed during thermal cycles. Absorptions due to BrOOBr and OBrBrO, which have also been proposed as intermediates of the BrO self-reaction, are not observed. Only small amounts of $BrBrO_2$ have been found, which are probably due to the direct reaction of Br_2 and O_2 in the course of the discharge and to the reaction of BrBrO and oxygen atoms during annealing. Furthermore, the hitherto unknown oxide $OBrBrO_2$ is most probably present in the matrixes after annealing, resulting from the reaction of oxygen atoms with $BrBrO_2$.

Acknowledgment. This research was supported by Hochschuljubiläumsstiftung der Stadt Wien, project H-847/2005, and the European Union, INTAS project 03-51-5698. A.L. acknowledges stipends from the Ausseninstitut, TU Vienna and VEWISTA. O.G. acknowledges financial support from the Spanish Ministerio de Educación y Ciencia, MEC. The authors would like to thank Philipp Baloh for his help concerning the experiments and spectra acquisition.

References and Notes

(1) Molina, L. T.; Molina, M. J. *J. Geophys. Res.* **1986**, *91*, 14501−14508.
(2) Solomon, S.; Garcia, R. R.; Rowland, F. S.; Wuebbles, D. J. *Nature (London)* **1986**, *321*, 755−758.
(3) Barrie, L. A.; Bottenheim, J. W.; Schnell, R. C.; Crutzen, P. J.; Rasmussen, R. A. *Nature (London)* **1988**, *224*, 134−141.
(4) Bottenheim, J. W.; Fuentes, J. D.; Tarasick, D. W.; Anlauf, K. G. *Atmos. Environ.* **2002**, *36*, 2535−2544.
(5) Haussmann, M.; Platt, U. *J. Geophys. Res.* **1994**, *99*, 25399−25413.
(6) Escribano, R.; Mosteo, R. G.; Gómez, P. C. *Can. J. Phys.* **2001**, *79*, 597−609.
(7) Wayne, R. P.; Poulet, G.; Biggs, P.; Burrows, J. P.; Cox, R. A.; Crutzen, P. J.; Hagman, G. D.; Jenkin, M. E.; Le Bras, G.; Moorgat, G. K.; Platt, U.; Schindler, R. N. *Atmos. Environ.* **1995**, *29*, 2675−2883.
(8) Yagi, K.; Williams, J.; Wang, N. Y.; Cicerone, R. J. *Science* **1995**, *267*, 1979−1981.
(9) Wennberg, P. O.; Cohen, R. C.; Stimpfle, R. M.; Koplow, J. P.; Anderson, J. G.; Salawitch, R. J.; Fahey, D. W.; Woodbridge, E. L.; Keim, E. R.; Gao, R. S.; Webster, C. R.; May, R. D.; Toohey, D. W.; Podolske, J. R.; Chan, K. R.; Wofsy, S. C. *Science* **1994**, *266*, 398−404.
(10) Platt, U.; Hönninger, G. *Chemosphere* **2003**, *52*, 325−338.
(11) Chase, M. W., Jr. *J. Phys. Chem. Ref. Data* **1996**, *25*, 1069−1111.
(12) Escribano, R.; Ortega, I. K.; Mosteo, R. G.; Gómez, P. C. *Can. J. Phys.* **2004**, *82*, 998−1005.
(13) Seppelt, K. *Acc. Chem. Res.* **1997**, *30*, 111−113.
(14) Hwang, I.-C.; Kuschel, R.; Seppelt, K. *Z. Anorg. Allg. Chem.* **1997**, *623*, 379−383.
(15) Müller, H. S. P.; Cohen, E. A. *J. Chem. Phys.* **1997**, *106*, 8344−8254.
(16) Müller, H. S. P.; Miller, C. E.; Cohen, E. A. *J. Chem. Phys.* **1997**, *107*, 8292−8302.
(17) Vayda, W. M. *Proc. Indian Acad. Sci.* **1937**, *6A*, 122−128.
(18) Vayda, W. M. *Proc. Indian Acad. Sci.* **1938**, *7A*, 321−326.
(19) Schwarz, R.; Schmeisser, M. *Ber. Dtsch. Chem. Ges.* **1937**, *70B*, 1163−1166.
(20) Rabinowitch, E.; Wood, W. C. *Trans. Faraday Soc.* **1936**, *32*, 907−917.
(21) Zintl, E.; Rienacker, G. *Ber. Dtsch. Chem. Ges.* **1930**, *63B*, 1098−1104.
(22) Dixon, D. A.; Parrish, D. D.; Herschbach, D. R.*Faraday Discuss. Chem. Soc.* **1973**, *55*, 385−387.
(23) Parrish, D. D.; Herschbach, D. R. *J. Chem. Soc.* **1973**, *95* (18), 6133−6134.
(24) Pacios, L. F.; Gómez, P. C. *THEOCHEM* **1999**, *467*, 223−231.
(25) Guha, S.; Francisco, J. S. *J. Phys. Chem. A* **1997**, *101*, 5347−5359.
(26) Li, Z.; Francisco, J. S. *Chem. Phys. Lett.* **2002**, *354*, 109−119.
(27) Guha, S.; Francisco, J. S. *J. Phys. Chem. A* **1998**, *102*, 6702−6705.
(28) Pak, C.; Xie, Y.; Schaefer, H. F., III *Mol. Phys.* **2003**, *101* (1−2), 211−225.
(29) Pacios, L. F.; Gómez, P. C. *J. Phys. Chem. A* **1997**, *101*, 1767−1773.
(30) Li, Z.; Jeong, G.-R. *Chem. Phys. Lett.* **2001**, *340*, 194−204.
(31) Kuschel, R.; Seppelt, K. *Angew. Chem.* **1993**, *105*, 1734−1735.
(32) Leopold, D.; Seppelt, K. *Angew. Chem.* **1994**, *106*, 1043−1044.
(33) Li, Z.; Jeong, G.-R.; Person, E. *Int. J. Chem. Kinet.* **2002**, *34*, 430−437.
(34) Tevault, D. E.; Walker, N.; Smardzewski, R. R.; Fox, W. B. *J. Phys. Chem.* **1978**, *82*, 2728−2733.
(35) Tevault, D. E.; Smardzewski, R. R. *J. Am. Chem. Soc.* **1978**, *100*, 3955−3957.
(36) Loewenschuss, A.; Miller, J. C.; Andrews, L. *J. Mol. Spectrosc.* **1980**, *81*, 251−262.
(37) Kölm, J.; Engdahl, A.; Schrems, O.; Nelander, B. *Chem. Phys.* **1997**, *214*, 313−319.
(38) Kölm, J.; Schrems, O.; Beichert, P. *J. Phys. Chem. A* **1998**, *102*, 1083−1089.
(39) Li, Z. *J. Phys. Chem. A* **1999**, *103*, 1206−1213.
(40) Mauldin, R. L., III; Wahner, A.; Ravishankara, A. R. *J. Phys. Chem.* **1993**, *97*, 7585−7596.
(41) Knight, G.; Ravishankara, A. R.; Burkholder, J. B. *J. Phys. Chem. A* **2000**, *104*, 11121−11125.
(42) Kopitzky, R.; Grothe, H.; Willner, H. *Chem.—Eur. J.* **2002**, *8*, 5601−5621.
(43) Pflugmacher, A. *Z. Anorg. Allg. Chem.* **1953**, *273*, 41−47.
(44) Frisch, M. J.; Trucks, G. W.; Schlegel, H. B.; Scuseria, G. E.; Robb, M. A.; Cheeseman, J. R.; Montgomery, J. A., Jr.; Vreven, T.; Kudin, K. N.; Burant, J. C.; Millam, J. M.; Iyengar, S. S.; Tomasi, J.; Barone, V.; Mennucci, B.; Cossi, M.; Scalmani, G.; Rega, N.; Petersson, G. A.; Nakatsuji, H.; Hada, M.; Ehara, M.; Toyota, K.; Fukuda, R.; Hasegawa, J.;

Ishida, M.; Nakajima, T.; Honda, Y.; Kitao, O.; Nakai, H.; Klene, M.; Li, X.; Knox, J. E.; Hratchian, H. P.; Cross, J. B.; Bakken, V.; Adamo, C.; Jaramillo, J.; Gomperts, R.; Stratmann, R. E.; Yazyev, O.; Austin, A. J.; Cammi, R.; Pomelli, C.; Ochterski, J. W.; Ayala, P. Y.; Morokuma, K.; Voth, G. A.; Salvador, P.; Dannenberg, J. J.; Zakrzewski, V. G.; Dapprich, S.; Daniels, A. D.; Strain, M. C.; Farkas, O.; Malick, D. K.; Rabuck, A. D.; Raghavachari, K.; Foresman, J. B.; Ortiz, J. V.; Cui, Q.; Baboul, A. G.; Clifford, S.; Cioslowski, J.; Stefanov, B. B.; Liu, G.; Liashenko, A.; Piskorz, P.; Komaromi, I.; Martin, R. L.; Fox, D. J.; Keith, T.; Al-Laham, M. A.; Peng, C. Y.; Nanayakkara, A.; Challacombe, M.; Gill, P. M. W.; Johnson, B.; Chen, W.; Wong, M. W.; Gonzalez, C.; Pople, J. A. *Gaussian 03*; Gaussian, Inc.: Wallingford, CT, 2004.

(45) Drouin, B. J.; Miller, C. E.; Müller, H. S. P.; Cohen, E. A. *J. Mol. Spectrosc.* **2001**, *205*, 128−138.

(46) Pacios, L. F.; Gómez, P. C. *Chem. Phys. Lett.* **1998**, *298*, 412−418.

(47) Thirugnanasambandam, P.; Mohan, S. *Indian J. Phys.* **1978**, *52B*, 173−178.

(48) Müller, H. S. P.; Miller, C. E.; Cohen, E. A. *Angew. Chem., Int. Ed. Engl.* **1996**, *35*, 2129−2131.

(49) Miller, C. E.; Nicolaisen, S. L.; Francisco, J. S.; Sander, S. P. *J. Chem. Phys.* **1997**, *107*, 2300−2307.

(50) Lee, M. *J. Phys. Chem.* **1996**, *100*, 19847−19852.

(51) Kwabia Tchana, F.; Orphal, J.; Kleiner, I.; Rudolph, H. D.; Willner, H.; Garcia, P.; Bouba, O.; Demaison, J.; Redlich, B. *Mol. Phys.* **2004**, *102* (14−15), 1509−1521.

(52) Scheffler, D.; Grothe, H.; Willner, H.; Frenzel, A.; Zetzsch, C. *Inorg. Chem.* **1997**, *36*, 335−338.

(53) Scheffler, D.; Willner, H. *Inorg. Chem.* **1998**, *37*, 4500−4506.

(54) Zoug, P.; Derecskei-Kovacs, A.; North, S. W. *J. Phys. Chem. A* **2003**, *107*, 888−896.

(55) Casper, B.; Lambotte, P.; Minkwitz, R.; Oberhammer, H. *J. Phys. Chem.* **1993**, *97*, 9992−9995.

(56) Wilson, W. W.; Christe, K. O. *Inorg. Chem.* **1987**, *26*, 1573−1580.

(57) Burkholder, J. B.; Hammer, P. D.; Howard, C. J.; Maki, A. G.; Thompson, G.; Chackerian, C., Jr. *J. Mol. Spectrosc.* **1987**, *124*, 139−161.

(58) Orlando, J. J.; Burkholder, J. B.; Bopegedera, A. M. R. P.; Howard, C. J. *J. Mol. Spectrosc.* **1991**, *145*, 278−289.

(59) Maier, G.; Bothur, A. *Z. Anorg. Allg.* **1995**, *621*, 743−746.

(60) Odeh, I. N.; Nicoson, J. S.; Hartz, K. E.; Margerum, D. W. *Inorg. Chem.* **2004**, *43*, 7412−7420.

(61) Nakata, M.; Somura, Y.; Takayanagi, M.; Tanaka, N.; Shibuya, K.; Uchimaru, T.; Tanabe, K. *J. Phys. Chem.* **1996**, *100*, 15815−15820.

(62) St. Louis, R. V.; Crawford, B., Jr. *J. Chem. Phys.* **1965**, *42*, 857−864.

(63) Hallamasek, D.; Babka, E.; Knözinger, E. *J. Mol. Struct.* **1997**, *408/409*, 125−132.

(64) Pascal, J. L.; Pavia, A. C.; Potier, J.; Potier, A. *C. R. Acad. Sci., Ser. C* **1974**, *279* (1), 43−46.